

# PREDICTING THE OCCURRENCE OF SURPLUS AND DEFICIT NET RADIATION IN IBADAN, NIGERIA

Agada, I.O.<sup>1</sup>, Udochukwu, B.C.<sup>2</sup>, and Sombo, T.<sup>3</sup>.

<sup>1,2,3</sup> Department of Physics, University of Agriculture, Makurdi. P.M.B 2373, Benue State, Nigeria

\*Corresponding Author Email Address: [gadexx@yahoo.com](mailto:gadexx@yahoo.com)

Phone: +2348034554084

## ABSTRACT

This study aims at predicting the occurrence of surplus and deficit net radiation in Ibadan, Nigeria. Thirty-four (34) years data (1977-2010) on daily maximum and minimum Relative-Humidity, Solar irradiance and maximum and minimum Air temperature were sourced from the International Institute of Tropical Agriculture (IITA) and used in the analysis. The Penman-Monteith (FAO-56) step by step method was used to compute net radiation in Ibadan. A two – state (surplus and deficit net radiation) Markov Chain model was developed and used in this work. The monthly transition counts, transition probability matrix, n-step transition matrix (power matrix), steady state probability vector and the vector of mean reoccurrence times (in days) were determined each for the two states. The model was also used in predicting the chance occurrence of surplus and deficit net radiation for one year. The average monthly net radiation is surplus (positive) in the months of February, March, April, May, June, October, November and December, while it is deficit (negative) in January, July, August, and September. The study also reveals a 69%, 76%, 76%, 74%, 63%, 63%, 70% and 52% chance occurrence of surplus net radiation in the months of February, March, April, May, June, October, November and December, while a 54%, 64%, 76% and 55% chance of deficit net radiation occurring in the months of January, July, August and September respectively using the Markov Chain model (steady states probabilities). The mean reoccurrences times (in days) analysis reveals that, on the average it takes: 1.4 days for surplus net radiation and 3.5 days for deficit net radiation to reoccur in the months of February, March, April, May, June, October, November and December; 3.9 days for deficit net radiation and 1.3 days for surplus net radiation to reoccur in the months of January, July, August and September. This explains why the air temperature of Ibadan is warmer in the months of February, March, April, May, June, October, November and December, and colder in January, July, August and September. The weather/climate is extremely warm in March and April, and extremely cold in August as revealed by the proportions of surplus and deficit net radiation for each month of the year.

**Keywords:** Net Radiation, surplus, deficit, Penman-Monteith (FAO-56), Markov Chain

## 1. INTRODUCTION

Net radiation is the basic factor that governs the climate of the troposphere (lower layers of the atmosphere). It is the difference between the incoming net shortwave radiation ( $R_s$ ) and the outgoing net longwave radiation ( $R_l$ ) (Lincoln et al., 2015). Surplus net radiation occurs when the total amount of incoming net shortwave radiation is greater than outgoing net longwave radiation while deficit net radiation occurs when the outgoing net longwave radiation is greater than the incoming net shortwave

radiation. In order to attain heat balance (surplus equal to deficit net radiation), the earth must emit the equivalent amount of energy absorbed back to space or else, the earth's temperature would rapidly rise or fall. A deviation in net radiation can cause the earth's air temperature to become warmer or cooler, resulting to various changes in lower atmosphere, ocean and land (U.S.E.P.A., 2014).

Air temperature is controlled by the total amount, duration and intensity of solar radiation that is absorb and the total terrestrial radiation that is emitted and re-absorb by the earth's surface. Increase in air temperature can result to extreme weather events such as intense rainfall, severe heat, drought, serious flooding, and violent storm, to mention few (O'Hare, 2002). According to Baldwin et al., (1971), extreme weather impact is one of the main factor causing setback and cost overruns on construction projects. Extreme weather tends to reduce labour productivity or stoppage of work, that is, reduced human performance due to extreme heat or cold stresses. Increase in solar radiation results in the increase of net radiation (surplus), which in turn affect air temperature. Solar radiation is one of the major component crops need for photosynthesis, surplus or deficit net radiation can also affect crops positively or negatively. According to Santillán-Soto et al., (2015), net radiation has a major influence on thermal comfort and harmful health effects on humans.

One key factor controlling evapotranspiration (evaporation and transpiration processes occurring simultaneously), climate change, yield of crops, weather forecasting, to mention a few, is the net radiation (Bennie et al., 2008; Ji et al., 2009; Li et al., 2009). In agrometeorology, net radiation is one of the main parameter generally used in estimating reference evapotranspiration and leaf wetness period in physical models (Allen et al., 2007). Despite its significance, most of the Automatic Meteorological Stations (AMS) do not measure net radiation ( $R_n$ ) directly because net radiometers are expensive instruments and require constant care in the field (Geraldo-Ferreira, 2011). Hence, it must be calculated by physical models.

Diverse authors have estimated and predicted net radiation using incoming solar (shortwave) radiation data. The simple linear regression (classical) method has being most successful (Neilsen et al., 1981; Pereira et al., 2007; Heldwein et al., 2012). Carrasco and Ortega-Farías, (2008) evaluated two simple models ( $R_{ne1}$  and  $R_{ne2}$ ) for estimating net radiation over a drip-irrigated Cabernet Sauvignon vineyard, trained on a vertical shoot-positioned system. They suggested that the proposed model  $R_{ne2}$  (assuming a temperature gradient between the canopy and air is not equal to zero) can be used to estimate net radiation, using air temperature, relative humidity and solar radiation as input data instead of the  $R_{ne1}$  (assuming a temperature gradient between the canopy and air is equal to zero) model. Mahalakshmia et al., (2014) applied Artificial Neural Network (ANN) method in

estimating net surface radiation from Terra MODIS data. The result reveals that the net surface radiation was estimated with a root mean square accuracy of 64w/m<sup>2</sup> and the square of the correlation coefficient (R<sup>2</sup>) was 0.75 or 75%. Danilton et al., (2018) used two empirical methods (Gauss and Practical) in estimating reference surface Net Radiation from Solar Radiation. The result obtained reveals that Gauss and Practical methods provides satisfactory results, with relative mean absolute error values less than 5.8%. Santiago et al., (2002) and Gavilán et al., (2007) recommended the use of Penman Monteith (FAO-56) model in computing net radiation (R<sub>n</sub>), given that Von Randow and Alvalá, (2006) and Galvão and Fisch, (2000) encounter difficulties in estimating net longwave (terrestrial) radiation employing the FAO-24 equation.

This study differs from the above mentioned works, as none of them modeled the chance occurrence of the surplus and deficit states of net radiation after computing net radiation. The stochastic nature of net radiation, as well as the significant role of the dynamics of surplus and deficit net radiation in the Global Circulation Heat Balance informed the adoption of the discrete time Markov Chain model in this work. The Markov Chain model was used in predicting the chance of surplus and deficit net radiation as well as their respective mean reoccurrence times.

## 1.1. Theoretical Framework

### 1.1.1. Penman-Monteith (FAO-56) Model

Due to high cost and constant maintenance of recording instruments such as net radiometers, net radiation (R<sub>n</sub>) measurements are difficult to collect. The Penman-Monteith (FAO-56) step by step method was used to compute the daily net radiation. This includes:

The inverse relative distance Earth-Sun ( $\partial r$ ) is given as (Spencer, 1971):  $\partial r = 1 + 0.033 \cos[\frac{2\pi}{365} j]$  (1)

where  $j$  is number of the day in the year between 1 (1 January) and 365 or 366 (31 December).

The solar declination ( $\delta$ ) can be found from the approximate equation of Cooper (1969),

$$\delta = 23.45 \sin(360 \frac{284 + j}{365})$$
 (2)

The sun angle ( $\omega_s$ ) is given by (John and William, 2013):

$$\omega_s = \arccos[-\tan(\phi) \tan(\delta)]$$
 (3)

where  $\phi$  is the latitude of a particular location.

The extraterrestrial radiation (R<sub>a</sub>), for each day of the year can be estimated using;

$$R_a = \frac{24 \times 3600}{\pi} G_{sc} \partial r$$
 (4)

$$(\cos \phi \cos \delta \sin \omega_s + \frac{\pi \omega_s}{180} \sin \phi \sin \delta)$$

where  $G_{sc}$  is solar constant given as 1367w/m<sup>2</sup> (Iqbal, 1983).

The actual vapor pressure ( $e_a$ ) can be computed (Lincoln et al., 2015);

$$e_a = \frac{e_{(T_{min})} [\frac{RH_{max}}{100}] + e_{(T_{max})} [\frac{RH_{min}}{100}]}{2}$$
 (5)
$$e_{(T_{max})} = 0.6108 \exp(\frac{17.27T_{max}}{T_{max} + 237.3})$$

$$e_{(T_{min})} = 0.6108 \exp(\frac{17.27T_{min}}{T_{min} + 237.3})$$

where  $e_{(T_{min})}$  and  $e_{(T_{max})}$  are daily saturation vapour pressure at minimum and maximum temperature, and  $RH_{max}$ ,  $RH_{min}$  are maximum and minimum relative humidity.

The clear-sky radiation  $R_{so}$  is given by (Lincoln et al., 2015):

$$R_{so} = (0.75 + 2E10 - 5Z)R_a$$
 (6)

where Z is the elevation above sea level.

The net terrestrial (long wave) radiation ( $R_T$ ) is proportional to the absolute temperature of the surface raised to the fourth power. This relation is expressed quantitatively by the Stefan-Boltzmann law as given below:

$$R_T = \sigma [\frac{(T_{max} + 273.16)^4 + (T_{min} + 273.16)^4}{2}]$$
 (7)
$$(0.34 - 0.14\sqrt{e_a})[1.35 \frac{R_s}{R_{so}} - 0.35]$$

where  $\sigma$  is Stefan-Boltzmann constant [4.903x10<sup>-9</sup>MJ K<sup>-4</sup> m<sup>-2</sup>day<sup>-1</sup>] and  $R_s$  is incoming solar radiation, MJm<sup>-2</sup> day<sup>-1</sup>.

Lastly, the net radiation ( $R_n$ ) which is the difference between the incoming net shortwave radiation ( $R_{ns}$ ) and the outgoing net terrestrial radiation ( $R_T$ ) is given by;

$$R_n = R_{ns} - R_T$$
 (8)

$$R_{ns} = (1 - a)R_s$$
 (9)

where  $R_{ns}$  is net solar radiation (MJ m<sup>-2</sup> day<sup>-1</sup>) and  $a$  is albedo given as 0.3 (John and Willam, 2013)

### 1.1.2. Markov Chain

Markov chain is a stochastic process  $\{X_n, n = 0, 1, 2, \dots\}$  that takes on a finite or countable number of possible values, if  $X_n = i$ , then the process is said to be in state  $i$  at time  $n$ . Supposing that the process is in state  $i$ , there is fixed probability  $P_{ij}$  that it will next be in state  $j$ . That is;

$$P\{X_{n+1} = j | X_n = i, X_{n-1} = i_{n-1}, \dots, X_1 = i_1, X_0 = i_0\} = P\{X_{n+1} = j | X_n = i\} = P_{ij}$$
 (10)

For all states  $i_0, i_1, \dots, i, j$  and  $n \geq 0$ .

For a first-order Markov chain, the future state  $X_{n+1}$  is independent of the previous states ( $X_0, X_1, \dots, X_{n-1}$ ), but depends only on the present state  $X_n$  (Ross, 2010).

### 1.1.3. Transition Probability Matrix

A Markov chain transition matrix is a square array describing the probabilities of the chain transiting from one state to another. This transition probability  $P_{ij}$  is given as (Balzter, 2000):

$$P_{ij} = \begin{pmatrix} P_{11} & P_{12} & \dots & P_{1n} \\ P_{21} & P_{22} & \dots & P_{2n} \\ \dots & \dots & \dots & \dots \\ P_{n1} & P_{n2} & \dots & P_{nn} \end{pmatrix} \quad (11)$$

The elements  $P_{ij}$  are also called stationary probabilities. They are defined by

$$P(X_n = j / X_{n-1} = i) = P_{ij} \quad (12)$$

Considering the long period of the daily net radiation (34 years) used in this work, the  $P_{ij}$ 's are assumed stationary.

#### 1.1.4. N-Step Transition Probability Matrix

For any value of  $n$  ( $n = 2, 3 \dots$ ), the  $n^{\text{th}}$  power of the matrix  $P$  specify the probabilities  $p_{ij}^n$  that the chain will move from state  $x_i$  to  $x_j$  is called the n-step probability matrix. This is based on the Chapman Kolmogorov equation, which states as follows; For any  $r \leq n$ ,

$$P_n = (P_{ij})_n = P^{(n)} = \sum_{k=0}^{\infty} P_{ik}^r P_{kj}^{n-r} \quad (13)$$

where  $P_n$  denotes the matrix of n-step transition probability (Udom, 2010)

#### 1.1.5. Steady State Probabilities of a Markov Chain

Consider a Markov chain with Z-states and the row vector  $\pi = (\pi_1 \pi_2 \dots \dots \dots \pi_z)$  (14)

$$\text{such that (i) } \pi_i \geq 0 \text{ (ii) } \sum_{i=1} \pi_i = 1 \text{ (iii) } \pi_j = \lim_{n \rightarrow \infty} p_{ij}^n \quad (15)$$

where  $(\pi_1, \pi_2, \dots \dots \dots \pi_z)$  is called the steady state vector of the Markov Chain.  $\pi$  can be obtained by solving the relation;

$$\pi = \pi P_{ij} \quad (16)$$

where  $P_{ij}$  are the stationary probabilities.

In this study, the steady state probabilities for the first order Markov chain model were determined using the computational formula:

$$\pi_1 = \frac{P_{01}}{1 + p_{01} - p_{11}} \quad (17)$$

$$\pi_2 = 1 - \pi_1 \quad (18)$$

$$1 = \pi_1 + \pi_2 \quad (19)$$

Where  $\pi_1$  and  $\pi_2$  are the steady state probabilities of surplus and deficit occurrence.

The mean recurrence time (in days) for each state is modeled as:

$$\frac{1}{\pi_1} \text{ and } \frac{1}{\pi_2} \quad (20)$$

## 2. METHODOLOGY

### 2.1. Source of Data

The daily maximum and minimum relative-humidity, maximum and minimum air temperature and solar radiation data were obtained from the International Institute of Tropical Agriculture (IITA) Ibadan, Nigeria for the period of thirty-four (34) years (1977-2010). The daily data were used in computing the daily actual vapor pressure ( $e_a$ ) and terrestrial (long wave) radiation ( $R_T$ ). The daily inverse relative distance earth-sun ( $\hat{r}$ ), solar declination ( $\delta$ ), sun angle ( $\omega_s$ ), extraterrestrial radiation ( $R_a$ )

, clear sky solar radiation ( $R_{so}$ ), and net radiation ( $R_n$ ) were also computed using the step by step Penman-Monteith model (equation 1-9). Lastly, the daily net radiation was arranged monthly over the period of the thirty four years (1977-2010) and the monthly averages were computed.

### 2.2. Source of Data

The daily net radiation over the period was transformed into sequence of binary events as follows. For any  $K^{\text{th}}$  day, a random variable  $X_k$  is defined to represent this event with the realization; '0' if the daily net radiation ( $R_n$ ) is negative (deficit) and '1' if the daily net radiation ( $R_n$ ) is positive (surplus). The random variable  $R_{nk}$  for net radiation is therefore defined as;

$$R_{nk} = \begin{cases} 0, & \text{if } R_{nk} < 0 \text{ (deficit net radiation).} \\ 1, & \text{if } R_{nk} > 0 \text{ (surplus net radiation).} \end{cases} \quad (21)$$

where  $k$  is 1, 2, ...,  $n$  (Days).

The Microsoft Excel Package was used to transform the computed daily net radiation into sequence of binary events using equation (21). Due to the huge amount of data involved in this work, a computer program was written in Pascal programming language version 1.5 for obtaining the transition counts, transition probabilities, N-step transition matrix and steady state probabilities using equation 10-18.

## 3. RESULTS AND DISCUSSION

### 3.1. Monthly net radiation

As a result of the absorption of incoming solar radiation in the atmosphere and on the earth surface, the earth surface gains energy that is converted to heat and emits it as terrestrial (long-wave) radiation back into the atmosphere. From Figure 1, the maximum average monthly net radiation occurs in the month of April, while the minimum was observed in August. This result agrees with the work of Sanusi and Abisoye (2011), they observed that two major maximum solar radiations occur in the dry season (April and November) and minimum solar radiation in the rainy season (August) at Ibadan. The average monthly net radiation is surplus (positive) in the months of February, March, April, May, June, October, November and December, while it is deficit (negative) in January, July, August and September as presented in Figure 1. This implies that the amount of incoming

solar radiation absorbed in months of February, March, April, May, June, October, November and December is higher compared to the amount of terrestrial radiation emitted by the earth's surface (Ibadan). Similarly, the amount of terrestrial radiation emitted in the months of January, July, August and September is higher compared to total amount of absorbed solar radiation.

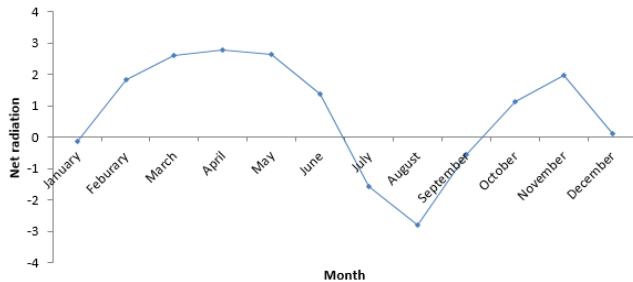


Figure 1: Average monthly Net radiation

Net radiation determines the weather / climate of a place. The air temperature at Ibadan is warmer in the months of February, March, April, May, June, October, November and December as a result of surplus net radiation, while it is cooler in January, July, August and September as a result of deficit net radiation. Since net radiation is almost zero in the months of January and December, the air temperature at Ibadan is not too the extreme when compared to the months of April and August as shown in Figure 1.

The surplus net radiation experienced in the months of February, March, April, May, June, October, November and December, heats up the water body, land surfaces and eventually evaporates moisture into the atmosphere in the form of sensible and latent heat. Thus, there is a net transfer of surplus energy to regions experiencing energy deficit to keep the air warm. This energy in the atmosphere is then released when water condenses, and warms the air in such regions. In order to keep the air warm in the months of January, July, August and September in Ibadan, surplus energy is transferred in the form of latent heat energy from regions experiencing surplus net radiation, this energy condenses to keep the atmosphere warm in these particular months. These transfer of energy by wind from one place to another helps to maintain thermal equilibrium on the earth's surface.

### 3.2. First order transition probability matrix

Formulating the transition probability matrix, the number of transitions from one state to other state was counted (transition counts) first as presented in Table 1.

Table 1: Monthly transition count for the various sequences

SEQ.	JAN.	FEB.	MAR.	APR.	MAY	JUNE	JULY	AUG.	SEPT.	OCT.	NOV.	DEC.
S-S	346	540	649	595	578	444	190	121	273	461	580	404
S-D	121	103	133	157	177	187	169	116	186	181	111	125
D-S	122	104	133	158	176	188	170	116	185	181	112	126
D-D	433	184	107	79	91	172	493	669	378	199	186	367

S-S- surplus net radiation day preceding surplus net radiation day  
 SEQ.-sequence

S-D- surplus net radiation day preceding deficit net radiation day

D-S- deficit net radiation day preceding surplus net radiation day

D-D- deficit net radiation day preceding deficit net radiation day

The transition probabilities of surplus net radiation transiting into surplus net radiation is higher in the months of February, March, April, May, June, October, November and December, while it is also observed that the transition probabilities of deficit net radiation transiting into deficit net radiation is higher in the months of January, July, August and September as shown in Figure 2.

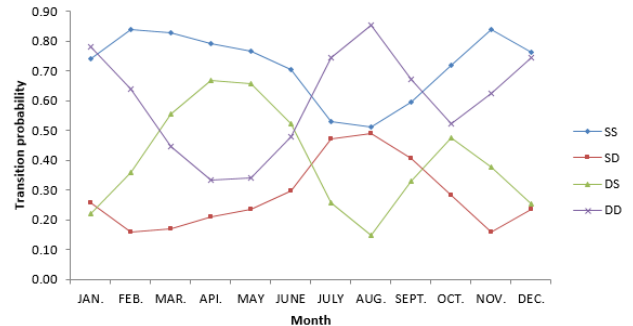


Figure 2: Monthly first order transition probabilities of surplus and deficit net radiation.

The transition probability of surplus net radiation transiting into surplus net radiation is the same in the months of February and November (0.84 or 84%). This implies that, there is a chance of 84% surplus net radiation occurring in the months of February and November, resulting to an extreme hot weather / climate at Ibadan, which agrees with Figure 1. Also there is 85% chance of deficit net radiation transiting into deficit net radiation in the month of August as presented in Figure 2. This signifies that, there is 85% chance of deficit net radiation occurring in the month of August, which explains why the month of August is extremely cool as shown in Figure 1.

### 3.3. N-Step Transition Probability

The n-step transition probability matrix provides idea of the long-term behavior of surplus and deficit net radiation. The elements of the n-step transition probability matrix  $P^n$  gives the probability of a current state transiting into another state after n-steps. The higher order of transition probabilities are computed by raising the power "n" of the matrix P. The daily predictions ( $P^{(2)} - P^{(31)}$ ) are the n-step transition probabilities of surplus and deficit net radiation occurring given the previous state as presented in tables 2 (a & b). If net radiation is in any of the two states, it will attain steady state when 'n' is equal to 13 (January), 10 (February), 6 (March), 4 (April), 3 (May), 5 (June, July and October), 9(August), 6(September), 11 (November) and 12 (December) as shown in table 2 (a & b). This refer to the fact that, the state of net radiation on an actual day is affected by the previous day (probabilities keep changing), but as the number of day's increases (n-power), the effect reduces resulting in a steady state.

**Table 2a:** Daily predictions of surplus and deficit net radiation from January to June.

Day	January		February		March		April		May		June	
	S	D	S	D	S	D	S	D	S	D	S	D
1	0.74	0.78	0.84	0.64	0.83	0.45	0.79	0.33	0.77	0.34	0.7	0.48
2	0.605	0.666	0.763	0.467	0.782	0.296	0.765	0.25	0.745	0.267	0.646	0.386
3	0.534	0.606	0.726	0.384	0.769	0.253	0.762	0.239	0.742	0.259	0.636	0.37
4	0.498	0.575	0.709	0.344	0.765	0.241	0.761	0.239	0.742	0.259	0.635	0.367
5	0.479	0.559	0.7	0.325	0.764	0.237	0.761	0.239	0.742	0.258	0.634	0.366
6	0.469	0.551	0.696	0.316	0.764	0.236	0.761	0.239	0.742	0.258	0.634	0.366
7	0.464	0.546	0.694	0.312	0.764	0.236	0.761	0.239	0.742	0.258	0.634	0.366
8	0.461	0.544	0.693	0.31	0.764	0.236	0.761	0.239	0.742	0.258	0.634	0.366
9	0.459	0.543	0.693	0.309	0.764	0.236	0.761	0.239	0.742	0.258	0.634	0.366
10	0.459	0.542	0.693	0.308	0.764	0.236	0.761	0.239	0.742	0.258	0.634	0.366
11	0.459	0.542	0.692	0.308	0.764	0.236	0.761	0.239	0.742	0.258	0.634	0.366
12	0.459	0.542	0.692	0.308	0.764	0.236	0.761	0.239	0.742	0.258	0.634	0.366
13	0.458	0.542	0.692	0.308	0.764	0.236	0.761	0.239	0.742	0.258	0.634	0.366
14	0.458	0.542	0.692	0.308	0.764	0.236	0.761	0.239	0.742	0.258	0.634	0.366
15	0.458	0.542	0.692	0.308	0.764	0.236	0.761	0.239	0.742	0.258	0.634	0.366
16	0.458	0.542	0.692	0.308	0.764	0.236	0.761	0.239	0.742	0.258	0.634	0.366
17	0.458	0.542	0.692	0.308	0.764	0.236	0.761	0.239	0.742	0.258	0.634	0.366
18	0.458	0.542	0.692	0.308	0.764	0.236	0.761	0.239	0.742	0.258	0.634	0.366
19	0.458	0.542	0.692	0.308	0.764	0.236	0.761	0.239	0.742	0.258	0.634	0.366
20	0.458	0.542	0.692	0.308	0.764	0.236	0.761	0.239	0.742	0.258	0.634	0.366
21	0.458	0.542	0.692	0.308	0.764	0.236	0.761	0.239	0.742	0.258	0.634	0.366
22	0.458	0.542	0.692	0.308	0.764	0.236	0.761	0.239	0.742	0.258	0.634	0.366
23	0.458	0.542	0.692	0.308	0.764	0.236	0.761	0.239	0.742	0.258	0.634	0.366
24	0.458	0.542	0.692	0.308	0.764	0.236	0.761	0.239	0.742	0.258	0.634	0.366
25	0.458	0.542	0.692	0.308	0.764	0.236	0.761	0.239	0.742	0.258	0.634	0.366
26	0.458	0.542	0.692	0.308	0.764	0.236	0.761	0.239	0.742	0.258	0.634	0.366
27	0.458	0.542	0.692	0.308	0.764	0.236	0.761	0.239	0.742	0.258	0.634	0.366
28	0.458	0.542	0.692	0.308	0.764	0.236	0.761	0.239	0.742	0.258	0.634	0.366
29	0.458	0.542	0.692	0.308	0.764	0.236	0.761	0.239	0.742	0.258	0.634	0.366
30	0.458	0.542			0.764	0.236	0.761	0.239	0.742	0.258	0.634	0.366
31	0.458	0.542			0.764	0.236			0.742	0.258		

**Table 2 b:** Daily predictions of surplus and deficit net radiation from July to December.

Day	July		August		September		October		November		December	
	S	D	S	D	S	D	S	D	S	D	S	D
1	0.53	0.74	0.51	0.85	0.59	0.67	0.72	0.52	0.84	0.62	0.76	0.74
2	0.403	0.67	0.422	0.611	0.483	0.584	0.653	0.405	0.766	0.445	0.64	0.61
3	0.369	0.651	0.27	0.777	0.456	0.562	0.637	0.377	0.733	0.365	0.58	0.545
4	0.36	0.646	0.247	0.77	0.448	0.556	0.633	0.371	0.716	0.328	0.55	0.512
5	0.357	0.644	0.239	0.767	0.447	0.555	0.632	0.369	0.709	0.311	0.535	0.496
6	0.356	0.644	0.236	0.767	0.446	0.554	0.632	0.369	0.707	0.303	0.528	0.488
7	0.356	0.644	0.235	0.766	0.446	0.554	0.632	0.368	0.705	0.299	0.524	0.484
8	0.356	0.644	0.235	0.766	0.446	0.554	0.632	0.368	0.704	0.298	0.522	0.482
9	0.356	0.644	0.234	0.766	0.446	0.554	0.632	0.368	0.704	0.297	0.521	0.481
10	0.356	0.644	0.234	0.766	0.446	0.554	0.632	0.368	0.704	0.297	0.52	0.481
11	0.356	0.644	0.234	0.766	0.446	0.554	0.632	0.368	0.704	0.296	0.52	0.481
12	0.356	0.644	0.234	0.766	0.446	0.554	0.632	0.368	0.704	0.296	0.52	0.48
13	0.356	0.644	0.234	0.766	0.446	0.554	0.632	0.368	0.704	0.296	0.52	0.48
14	0.356	0.644	0.234	0.766	0.446	0.554	0.632	0.368	0.704	0.296	0.52	0.48
15	0.356	0.644	0.234	0.766	0.446	0.554	0.632	0.368	0.704	0.296	0.52	0.48
16	0.356	0.644	0.234	0.766	0.446	0.554	0.632	0.368	0.704	0.296	0.52	0.48
17	0.356	0.644	0.234	0.766	0.446	0.554	0.632	0.368	0.704	0.296	0.52	0.48
18	0.356	0.644	0.234	0.766	0.446	0.554	0.632	0.368	0.704	0.296	0.52	0.48
19	0.356	0.644	0.234	0.766	0.446	0.554	0.632	0.368	0.704	0.296	0.52	0.48
20	0.356	0.644	0.234	0.766	0.446	0.554	0.632	0.368	0.704	0.296	0.52	0.48
21	0.356	0.644	0.234	0.766	0.446	0.554	0.632	0.368	0.704	0.296	0.52	0.48
22	0.356	0.644	0.234	0.766	0.446	0.554	0.632	0.368	0.704	0.296	0.52	0.48
23	0.356	0.644	0.234	0.766	0.446	0.554	0.632	0.368	0.704	0.296	0.52	0.48
24	0.356	0.644	0.234	0.766	0.446	0.554	0.632	0.368	0.704	0.296	0.52	0.48
25	0.356	0.644	0.234	0.766	0.446	0.554	0.632	0.368	0.704	0.296	0.52	0.48
26	0.356	0.644	0.234	0.766	0.446	0.554	0.632	0.368	0.704	0.296	0.52	0.48
27	0.356	0.644	0.234	0.766	0.446	0.554	0.632	0.368	0.704	0.296	0.52	0.48
28	0.356	0.644	0.234	0.766	0.446	0.554	0.632	0.368	0.704	0.296	0.52	0.48
29	0.356	0.644	0.234	0.766	0.446	0.554	0.632	0.368	0.704	0.296	0.52	0.48
30	0.356	0.644	0.234	0.766	0.446	0.554	0.632	0.368	0.704	0.296	0.52	0.48
31	0.356	0.644	0.234	0.766			0.632	0.368			0.52	0.48

**3.4. Steady state probabilities**

The monthly steady state probabilities (long run dependence) of surplus and deficit net radiation are presented in Figure 3. The surplus net radiation turns maxima in the months of March and November with probabilities of 0.76, and 0.70 respectively, while minima in the month of August with probability 0.23. It is observed that deficit net radiation turned maxima in the month of August with probability 0.77 and minima in the months of March and November with probabilities 0.24 and 0.30 respectively as shown in Figure 3.

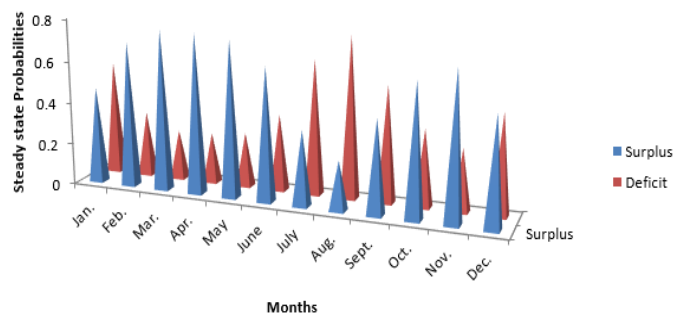


**Figure 3:** Monthly steady state probabilities of Surplus and deficit net radiation.

This implies that; there is a chance of 76% and 70% surplus net radiation, 24% and 30% deficit net radiation occurring in the months of March and November respectively, resulting to an increase in air temperature; a chance of 77% deficit net radiation and 23% surplus net radiation occurring in the month of August, resulting to a drastic reduction in air temperature. Thus, there is 69%, 76%, 76%, 74%, 63%, 63%, 70%, and 52% chance that net radiation would be surplus in the months of February, March, April, May, June, October, November and December respectively, while a 54%, 64%, 76% and 55% chance of net radiation been deficit in January, July, August and September as shown in Figure 3.

Huge amount of incoming solar radiation absorb by the earth's surface (Ibadan), results to surplus net radiation as seen in the months of February, March, April, May, June, October, November and December. The rainy season is characterized with clouds, which are very good reflector of incoming solar radiation back to space, which explains why the amount of terrestrial radiation emitted in the months of July, August and September is greater than the amount of solar radiation absorb resulting to a deficit net radiation. The month of January is so dry and cloud-free, but it is characterize with dust, which is also a good reflector of incoming solar radiation. Observe that Figures 1 only reflect the monthly distribution of surplus and deficit net radiation but did not reflect the proportions of variability. On the contrary, the steady state result of the Markov chain model as presented in Figure 3, did not only reflect the distribution, but also reflects the chances (proportions) of surplus and deficit net radiation for each month of the year.

### 3.5. Mean Reoccurrence Time (days)

The mean reoccurrence times (days) of surplus net radiation turned minima in months of March and November, while it became maxima in the month of August. Similarly, that of deficit net radiation turned minima in month of August and maxima in the months March and November as presented in Figure 4.

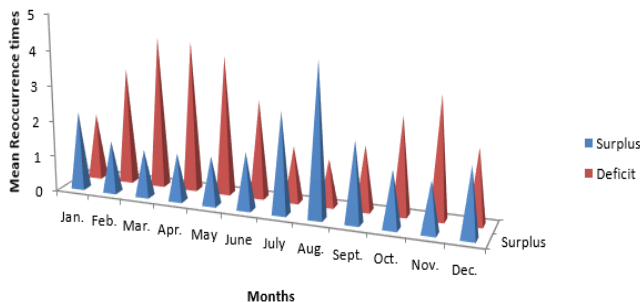


**Figure 4:** Monthly mean recurrence time (days) of Surplus and deficit net radiation.

It would take 1.3 and 4.2 days for a surplus and deficit net radiation state to reoccur in the month March, while 4.3 and 1.3 days for a deficit and surplus net radiation state to reoccur in August as shown in Figure 4. This indicates that, net radiation would be surplus for 4.2 days and deficit for 1.3 days in the month of March, whereas it would be deficit for 4.3 days and surplus for 1.3 days in August. This explains why the month of March is very hot and August very cool. It is also observed that, it would take 1.4 and 3.5 days on the average for a surplus and deficit net

radiation state to reoccur in the months of February, March, April, May, June, October, November and December, while 3.9 and 1.3 days on the average for a deficit and surplus net radiation state to reoccur in the months of January, July, August and September.

### 4. Conclusion

The following conclusions were drawn from the study:

- (i) The average monthly net radiation is surplus in the months of February, March, April, May, June, October, November and December, while it is deficit in January, July, August and September.
- (ii) The transition probabilities of surplus net radiation day preceding surplus net radiation day is higher in the months of February, March, April, May, June, October, November and December, while that of deficit net radiation day preceding deficit net radiation day is higher in January, July, August and September.
- (iii) There is 69%, 76%, 76%, 74%, 63%, 63%, 70%, and 52% chance that net radiation would be surplus in the month of February, March, April, May, June, October, November and December, while a 54%, 64%, 76% and 55% chance of it been deficit in the month January, July, August and September as revealed by the steady state probabilities.
- (iv) The mean reoccurrence times (days) revealed that, it would take 1.4 and 3.5 days on the average for a surplus and deficit net radiation state to reoccur in the months of February, March, April, May, June, October, November and December, while 3.9 and 1.3 days on the average for a deficit and surplus net radiation state to reoccur in the months of January, July, August and September.

### REFERENCES

Allen, R., Tasumi, M., Trezza, R., (2007). Satellite-based energy balance for mapping evapotranspiration with internalized calibration (metric)—Model. *J. Irrig. Drain. Eng.* 133, 380–394.

Balster, H., (2000). Markov chain models for vegetation dynamics. *Ecological Modelling*, 126(2):139(154), 2000.

Baldwin, J.R., Manthei, J.M., Rothbart, H., and Harris, R.B., (1971). Causes of delay in the construction industry. *ASCE Journal of the Construction Division*, 97: 177.187

Bennie, B. H. J., Wiltshire, A., Hill, M. O., Baxter, R., (2008). Slope, aspect and climate: Spatially explicit and implicit models of topographic microclimate in chalk grassland. *Ecological Modelling*, 216(1), 47–59.

Carrasco, M., Samuel, O., (2008). Evaluation of a model to simulate net radiation over a Vineyard cv. Cabernet Sauvignon. *Chilean journal of agricultural research* 68:156-165

Cooper, P. I., (1969). The Absorption of Solar Radiation in Solar Stills. *Journal of Solar Energy*, 12 (3).

Danilton, L. F., Maiara, K. A. R., Eder, C., Carlos, R. F., (2018). Empirical methods for estimating reference surface net radiation from solar radiation. *Engenharia Agrícola, Jaboticabal*, v.38, n.1, p.32-37.

- Gavilán, P., Berengena, J., Allen, R.G., (2007). Measuring versus Estimating Net Radiation and Soil Heat Flux: Impact on Penman-Monteith Reference ET Estimates in Semiarid Regions. *Agricultural Water Management*, **89**, 275-286.
- Galvão, J.A.C., Fisch, G., (2000). Radiation Balance in Pasture in the Amazon. *Revista Brasileira de Agrometeorologia*, **8**, 1-10.
- Geraldo-Ferreira, A., Soria-Olivas, E., Gómez-Sanchis, J., Serrano-López, A.J., Velázquez-Blázquez, A., López-Baeza, E., (2011). Modelling net radiation at surface using "in situ" netpyrriadiometer measurements with artificial neural networks. *Expert Systems with Applications* **38** 14190–14195.
- Heldwein, A.B., Maldaner, I.C., Bosco, L.C., Trentin, G., Grimm, E.L., Radons, S.Z., Pitol Lucas, D.D., (2012). Saldo de radiação diurno em dosséis de batata como função da radiação solar global. *Revista Ciência Agronômica* **3**(1):96-104.
- Iqbal, M., (1983). *An Introduction to Solar Radiation*, Academic, Toronto.
- John A. D., William A. B., (2013). *Solar Engineering of Thermal Processes Fourth Edition*. John Wiley & Sons, Inc. Published.
- Ji, X., Kang, E., Zhao, W., Zhang, Z., Jin, B., (2009). Simulation of heat and water transfer in a surface irrigated, cropped sandy soil. *Agricultural Water Management*, **96**(6), 1010–1020.
- Lincoln, Z., Michael, D. D., Consuelo, C. R., Kati, W. M., Kelly, T. M., (2015). Step by Step Calculation of the Penman-Monteith Evapotranspiration (FAO-56 Method). *Journal of Agricultural and Biological Engineering Department, UF/IFAS Extension*.
- Li, S., Tong, L., Li, F., Zhang, L., Zhang, B., Kang, S., (2009). Variability in Energy Partitioning and Resistance Parameters for a Vineyard in Northwest China. *Agricultural Water Management*, **96**(6), 955–962.
- Mahalakshmia, D.V., Arati Paul, D. D., Ali, M.M., Chandra S. J., Vinay, K. D., (2014). Net Surface Radiation Retrieval Using Earth Observation Satellite Data and Machine Learning Algorithm. *ISPRS Annals of the Photogrammetry, Remote Sensing and Spatial Information Sciences*, **2**(8).
- Neilsen, L.B., Prahm, L.P., Berkowicz, R., Conradse, K., (1981). Incoming radiation estimated from hourly global radiation cloud observations. *J. Climatol.* **1**, 255–272.
- Pereira, R.A., Angelocci, L.R., Sentelhas, P.C., (2007). *Meteorologia agrícola*. Piracicaba, ESALQ/USP. 192p.
- O'Hare, G., (2002). Climate Change and the Temple of Sustainable Development. *Geography*, **87**(3): 234-246.
- Ross, S., (2010). *Introduction to Probability Models*. Elsevier Inc., 10<sup>th</sup> edition.
- Santiago, A.V., Pereira, A.R., Folegatti, M.V., Maggiotto, S.R., (2002). Reference Evapotranspiration Measured with a Weighing Lysimeter and Estimated by Penman-Monteith (FAO-56) on a Monthly and Ten-Days Time Scales. *Revista Brasileira de Agrometeorologia*, **10**, 57-66.
- Sanusi, Y. K., Abisoye, S. G., (2011). Estimation of Solar Radiation at Ibadan, Nigeria. *Journal of Emerging Trends in Engineering and Applied Sciences (JETEAS)* **2** (4): 701-705.
- Santillán-Soto N., García-Cueto, R., Haro-Rincón, Z., Ojeda-Benítez, S., Quintero-Núñez, M., Velázquez-Limón, N., (2015). Radiation Balance of Urban Materials and Their Thermal Impact in Semi-Desert Region: Mexicali, México Study Case *Atmosphere* **6**, 1578-1589
- Spencer, J. W., (1971). Fourier Series Representation of the Position of the Sun. *Search*, **2** (5), pp172.
- Udom, A.U., (2010). *Elements of Applied Mathematical Statistics*. ICIDR Publishing House Akwa Ibom.
- U.S. Environmental Protection Agency, (2014). *Climate change indicators in the United States*, Third edition. [www.epa.gov/climatechange/indicators](http://www.epa.gov/climatechange/indicators).
- Von Randow, R.C.S., Alvalá, R.C.S., (2006). Estimation of Long-Wave Atmospheric Radiation over Pantanal Sul Mato Grossense during the Dry Seasons of 1999 and 2000. *Revista Brasileira de Meteorologia*, **21**, 398-412.